EUROPEAN LABORATORY FOR PARTICLE PHYSICS

LEPEWWG/FSI/2002-01
ALEPH 2002-027 PHYSIC 2002-016
DELPHI 2002-090 CONF-623
L3 Note 2768
OPAL TN-724
July 17th 2002

Combined Preliminary Results on Colour Reconnection Using Particle Flow in $e^+e^- \rightarrow W^+W^-$

The LEP Collaborations ALEPH, DELPHI, L3 and OPAL and the LEP W Working Group

Abstract

Measurements of the inclusive particle flow distributions in $e^+e^- \rightarrow W^+W^-$ events are used to search for the effects of colour reconnection. This note presents a first, preliminary combination of the measurements of the LEP Collaborations. The data are compared with various models implementing colour reconnection effects. The extreme scenario of the SK-I model of colour reconnection is ruled out and a limit on the model parameter controlling the fraction of reconnected events is set.

Prepared from contributions of the LEP Collaborations to the Summer 2002 conferences

1 Introduction

In $W^+W^- \rightarrow q\overline{q}q\overline{q}$ events, the products of the two (colour singlet) W decays in general have a significant space-time overlap as the separation of their decay vertices, $\tau_W \sim 1/\Gamma_W \approx 0.1$ fm, is small compared to characteristic hadronic distance scales of ~ 1 fm. Colour reconnection, also known as colour rearrangement (CR), was first introduced in [1] and refers to a reorganisation of the colour flow between the two W bosons. A precedent is set for such effects by colour suppressed B meson decays, *e.g.* $B \rightarrow J/\psi K$, where there is "cross-talk" between the two original colour singlets, $\bar{c}$+s and c+spectator [2].

QCD interference effects between the colour singlets in W^+W^- decays during the perturbative phase are expected to be small, affecting the W mass by $\sim (\frac{\alpha_S}{\pi N_{\mathrm{colours}}})^2 \Gamma_W \sim \mathcal{O}(1\ \mathrm{MeV})$ [2]. In contrast, non-perturbative effects involving soft gluons with energies less than Γ_W may be significant, with effects on $m_W \sim \mathcal{O}(10\ \mathrm{MeV})$. To estimate the impact of this phenomena a variety of phenomenological models have been developed [2–7], some of which are compared with data in this note.

Many observables have been considered in the search for an experimental signature of colour reconnection. The inclusive properties of events such as the mean charged particle multiplicity, distributions of thrust, rapidity, transverse momentum and $\ln(1/x_p)$ are found to have limited sensitivity [8–11]. The effects of CR are predicted to be numerically larger in these observables when only higher mass hadrons such as kaons and protons are considered [12]. However, experimental investigations [9,13] find no significant gain in sensitivity due to the low production rate of such species in W decays and the finite size of the data sample.

More recently, in analogy with the "string effect" analysis in 3-jet $e^+e^- \rightarrow q\overline{q}g$ events [14], the so-called "particle flow" method [15–17] has been investigated by all LEP collaborations [18–21]. In this, pairs of jets in $W^+W^- \rightarrow q\overline{q}q\overline{q}$ events are associated with the decay of a W and four jet-jet regions are chosen: two corresponding to jets sharing the same W parent (intra-W), and two in which the parents differ (inter-W).

Particles are projected onto the planes defined by these jet pairs and the particle density constructed as a function of ϕ, the projected angle relative to one jet in each plane. To account for the variation in the jet-jet opening angle, ϕ_0, the particle densities in ϕ are transformed into functions of a normalised angle, $\phi_r = \phi/\phi_0$, by a simple rescaling of the projected angle for each particle, event by event. Particles that in the plane of the jets have projected angles ϕ larger than ϕ_0 are not considered further. This gives particle densities, $\frac{1}{N_{\mathrm{event}}}\frac{\mathrm{d}n}{\mathrm{d}\phi_r}$, in four regions with ϕ_r in the range 0–1, and where n and N_{event} are the number of particles and events, respectively.

As particle density reflects the colour flow in an event, CR models predict a change in the relative particle densities between inter-W and intra-W regions. On average, colour reconnection is expected to affect the particle densities of both inter-W regions in the same way and so they are added together, as are the two intra-W regions. The observable used to quantify such changes, R_N, is defined:

$$R_N = \frac{\frac{1}{N_{\mathrm{event}}}\int_{0.2}^{0.8}\frac{\mathrm{d}n}{\mathrm{d}\phi_r}(\mathrm{intra-W})\mathrm{d}\phi_r}{\frac{1}{N_{\mathrm{event}}}\int_{0.2}^{0.8}\frac{\mathrm{d}n}{\mathrm{d}\phi_r}(\mathrm{inter-W})\mathrm{d}\phi_r}\,. \qquad (1)$$

As the effects of CR are expected to be enhanced for low momentum particles far from the jet axis, the range of integration excludes jet cores ($\phi_r \approx 0$ and $\phi_r \approx 1$). The precise upper and lower limits are optimised by model studies of predicted sensitivity.

Each LEP experiment has developed its own variation on this analysis, differing primarily in the selection of $\mathrm{W^+W^-} \to \mathrm{q\overline{q}q\overline{q}}$ events. In L3 [20] and DELPHI [19], events are selected in a very particular configuration ("topological selection") by imposing restrictions on the jet-jet angles and on the jet resolution parameter for the three- to four-jet transition (Durham or LUCLUS schemes). This leads to more planar events than those in an inclusive $\mathrm{W^+W^-} \to \mathrm{q\overline{q}q\overline{q}}$ sample and the association between jet pairs and W's is given by the relative angular separation of the jets. The overall efficiency for selecting events is $\sim 15\%$. The ALEPH [18] and OPAL [21] event selections are based on their W mass analyses. Assignment of pairs of jets to W's also follows that used in measuring m_{W}, using either a 4-jet matrix element [22] or a multivariate algorithm [23]. These latter selections have much higher efficiencies, varying ∼90–45%, but lead to samples of events having a less planar topology and hence a more complicated colour flow. ALEPH applies also the topological selection for consistency checks.

The data are corrected bin-by-bin for background contamination in the inter-W and intra-W regions separately. The possibility of CR effects existing in background processes, such as $\mathrm{ZZ} \to \mathrm{q\overline{q}q\overline{q}}$, is neglected. Since the data are not corrected for the effects of event selection, momentum resolution and finite acceptance, the values of R_N measured by the experiments cannot be compared directly with one another. However, it is possible to perform a relative comparison by using a common sample of Monte Carlo events, processed using the detector simulation program of each experiment.

2 Combination Procedure

The measured values of R_N can be compared after they have been normalised using a common sample of events, processed using the detector simulation and particle flow analysis of each experiment. A variable, r, is constructed:

$$r = \frac{R_N^{\mathrm{data}}}{R_N^{\mathrm{no-CR}}}, \tag{2}$$

where R_N^{data} and $R_N^{\mathrm{no-CR}}$ are the values of R_N measured by each experiment in data and in a common sample of events without CR. In the absence of CR, all experiments should find r consistent with unity. The default no-CR sample used for this normalisation consists of $\mathrm{e^+e^-} \to \mathrm{W^+W^-}$ events produced using the KORALW [24] event generator and hadronised using either JETSET [25], ARIADNE [26] or HERWIG [4] model depending on the tested fragmentation model. Input from experiments used to perform the combination is given in terms of R_N and detailed in Appendix A.

2.1 Weights

The statistical precision of R_N measured by the experiments does not reflect directly the sensitivity to CR, for example the measurements of ALEPH and OPAL have efficiencies several times larger than the topological selections of L3 and DELPHI, yet only yield comparable sensitivity. The relative sensitivity of the experiments may also be model dependent. Therefore, results are averaged using model dependent weights, *i.e.*

$$w_i = \frac{(R_N^i - R_N^{i,\mathrm{no-CR}})^2}{\sigma^2_{R_N}(\mathrm{stat.}) + \sigma^2_{R_N}(\mathrm{syst.})}\,, \tag{3}$$

where R_N^i and $R_N^{i,\mathrm{no-CR}}$ represent the R_N values for CR model i and its corresponding no-CR scenario, and $\sigma^2_{R_N}$ are the total statistical and systematic uncertainties. To test models, R_N values using common samples are provided by experiments for each of the following models:

1. SK-I, 100% reconnected (KORALW + JETSET),
2. AR-2 (KORALW + ARIADNE),
3. HERWIG CR, reconnected fraction $\frac{1}{9}$ (KORALW + HERWIG).

Samples in parentheses are the corresponding no-CR scenarios used to define w_i. These special Monte Carlo samples (called Cetraro samples) have been generated with the ALEPH tuned parameters, obtained with hadronic Z decays, and have been processed through the detector simulation of each experiment.

2.2 Combination of centre-of-mass energies

The common files required to perform the combination are only available at a single centre-of-mass energy (E_{cm}) of 188.6 GeV. The data from the experiments can only therefore be combined at this energy. The procedure adopted to combine all LEP data is summarised below.

R_N is measured in each experiment at each centre-of-mass energy, in both data and Monte Carlo. Using each experiment's own simulated $e^+e^- \rightarrow W^+W^-$ samples of JETSET No CR, the predicted variation of R_N with centre-of-mass energy is determined. This is parametrised by fitting a polynomial to these simulated R_N. The R_N measured in data are subsequently extrapolated to the reference energy of 189 GeV using this function, and the weighted average of the rescaled values in each experiment is used as input to the combination.

3 Systematics

Sources of systematic uncertainty are separated into correlated and uncorrelated sources between experiments. For correlated sources, the component correlated between all experiments is assigned as the smallest uncertainty found in any single experiment, with the quadrature remainder treated as an uncorrelated contribution. Preliminary estimates of the dominant systematics on R_N are given in Appendix A for each experiment, and described below. Additional common files are required for some of these to be treated properly.

3.1 Hadronisation

This is assigned by comparison of the single sample of $\mathrm{W^+W^-}$ events generated using KORALW, and hadronised with three different models, *i.e.* JETSET, HERWIG and ARIADNE. The systematic is assigned as the spread of the R_N values obtained when using the various models given in Appendix A. This is treated as a correlated uncertainty.

3.2 Bose-Einstein Correlations

Recent analyses [27–30] have shown no evidence for significant inter-W Bose-Einstein correlation (BEC) in $\mathrm{W^+W^-} \to \mathrm{q\overline{q}q\overline{q}}$ events. Therefore, BEC effects are only considered within each W separately. The estimated uncertainty is assigned, using common MC samples, as the difference in R_N between an intra-W BEC sample and the corresponding no-BEC sample. This is treated as correlated between experiments.

3.3 Background

Background is dominated by the $\mathrm{e^+e^-} \to \mathrm{q\overline{q}}$ process, with a smaller contribution from $\mathrm{ZZ} \to \mathrm{q\overline{q}q\overline{q}}$ diagrams. As no common background samples exist, apart from dedicated ones for BEC analyses, experiment specific samples are used. The uncertainty is defined as the difference in the R_N value relative to that obtained using the default background model and assumed cross-sections in each experiment.

3.3.1 $\mathrm{e^+e^-} \to \mathrm{q\overline{q}}$

The systematic is separated into two components, one accounting for the shape of the background, the other for the uncertainty in the value of the background cross-section, $\sigma(\mathrm{e^+e^-} \to \mathrm{q\overline{q}})$.

Uncertainty in the shape is estimated by comparing hadronisation models. Experiments typically have large samples simulated using 2-fermion event generators hadronised with various models. This uncertainty is assigned as $\pm\frac{1}{2}$ of the largest difference between any pair of hadronisation models and treated as uncorrelated between experiments.

The second uncertainty arises due to the accuracy of the experimentally measured cross-sections. The systematic is assigned as the larger of the deviations in R_N caused when $\sigma(\mathrm{e^+e^-} \to \mathrm{q\overline{q}})$ is varied by $\pm 10\%$ from its default value. This variation was based on the conclusions of a recent study comparing four-jet data with models [31], and is significantly larger than the $\sim 1\%$ uncertainty in the inclusive $e^+e^- \to q\overline{q}$ ($\sqrt{s'/s} > 0.85$) cross-section measured by the LEP2 2-fermion group. It is treated as correlated between experiments.

3.3.2 $ZZ \to q\overline{q}q\overline{q}$

Similarly to the $e^+e^- \to q\overline{q}$ case, this background cross-section is varied by $\pm 15\%$. For comparison, the uncertainty on $\sigma(ZZ)$ measured by the LEP2 4-fermion group is $\sim 11\%$ at $\sqrt{s} \simeq 189$ GeV. It is treated as correlated between experiments.

3.3.3 $W^+W^- \to q\overline{q}\ell\nu_\ell$

Semi-leptonic WW decays which are incorrectly identified as $W^+W^- \to q\overline{q}q\overline{q}$ events are the third main category of background, and its contribution is very small. The fraction of $W^+W^- \to q\overline{q}\ell\nu_\ell$ events present in the sample used for the particle flow analysis varies in the range 0.04–2.2% between the experiments. The uncertainty in this background consists of hadronisation effects and also uncertainty in the cross-section. As this source is a very small background relative to those discussed above, and the effect of either varying the cross-section by its measured uncertainty or of changing the hadronisation model do not change the measured R_N significantly, this source is neglected.

3.4 Detector Effects

The data are not corrected for the effects of finite resolution or acceptance. Various studies have been carried out, e.g. by analysing $W^+W^- \to q\overline{q}\ell\nu_\ell$ events in the same way as $W^+W^- \to q\overline{q}q\overline{q}$ events in order to validate the method and the choice of energy flow objects used to measure the particle yields between jets [20]. To take into account the effects of detector resolution and acceptance, ALEPH, L3 and OPAL have studied the impact of changing the object definition entering the particle flow distributions and have assigned a systematic error from the difference in the measured R_N.

3.5 Centre-of-mass energy dependence

As there may be model dependence in the parametrised energy dependence, the second order polynomial used to perform the extrapolation to the reference energy of 189 GeV is usually determined using several different models, with and without colour reconnection. DELPHI, L3 and OPAL use differences relative to the default no-CR model to assign a systematic uncertainty while ALEPH takes the spread of the results obtained with all the models with and without CR which have been used. This error is assumed to be uncorrelated between experiments.

3.6 Weighting function

The weighting function of Equation 3 could justifiably be modified such that only the uncorrelated components of the systematic uncertainty appear in the denominator. To accommodate this, the average is performed using both variants of the weighting function. This has an insignificant effect on the consistency between data and model under test, e.g. for SK-I the result is changed by 0.02σ, and this effect is therefore neglected.

4 Combined Results

Experiments provide their results in the form of R_N (or changes to R_N) at a reference centre-of-mass energy of 189 GeV by scaling results at various energies using the predicted energy dependence of their own non-CR MC samples. This avoids having to generate common samples at multiple centre-of-mass energies.

The detailed results from the participating experiments are included in Appendix A. These consist of preliminary results, taken from the publically available notes [18–21], and additional information from analysis of Monte Carlo samples. The averaging procedure itself is carried out by each of the experiments and good agreement is obtained.

An example of this averaging to test the SK-I CR model (full reconnection) is given in Appendix B. The average obtained in this case is:

$$\begin{aligned} r(data) &= 0.969 \pm 0.011(\text{stat.}) \pm 0.009(\text{syst.correl.}) \pm 0.006(\text{syst.uncorrel.})\,, \\ r(\text{SK-I }100\%) &= 0.8909\,. \end{aligned}$$

The measurements of each experiment and this combined result are shown in Figure 1. Thus the data disagree with the extreme scenario of this particular model at a level of 5.2σ of the total error. The data from the 4 experiments shown are consistent and tend to prefer an intermediate colour reconnection scenario than no colour reconnection at a 2σ level in the SKI framework.

4.1 Parameter space in SK-I model

In the SK-I model, the reconnection probability is governed by an arbitrary, free parameter, k_I. By comparing the data with model predictions evaluated at a variety of k_I values, it is possible to determine the reconnection probability that is most consistent with data, which can in turn be used to estimate the corresponding bias in the measured m_{W}. By repeating the averaging procedure using model inputs for the set of k_I values given in Table 2 it is found that the data prefer a value of k_I =1.18 as shown in Figure 2. The 68%CL lower and upper limits are 0.39 and 2.13 respectively. The LEP averages obtained for the different k_I values are summarised in Table 4. It corresponds to a preferred reconnection probability in this model at 189 GeV of 49% as can be seen from Figure 3.

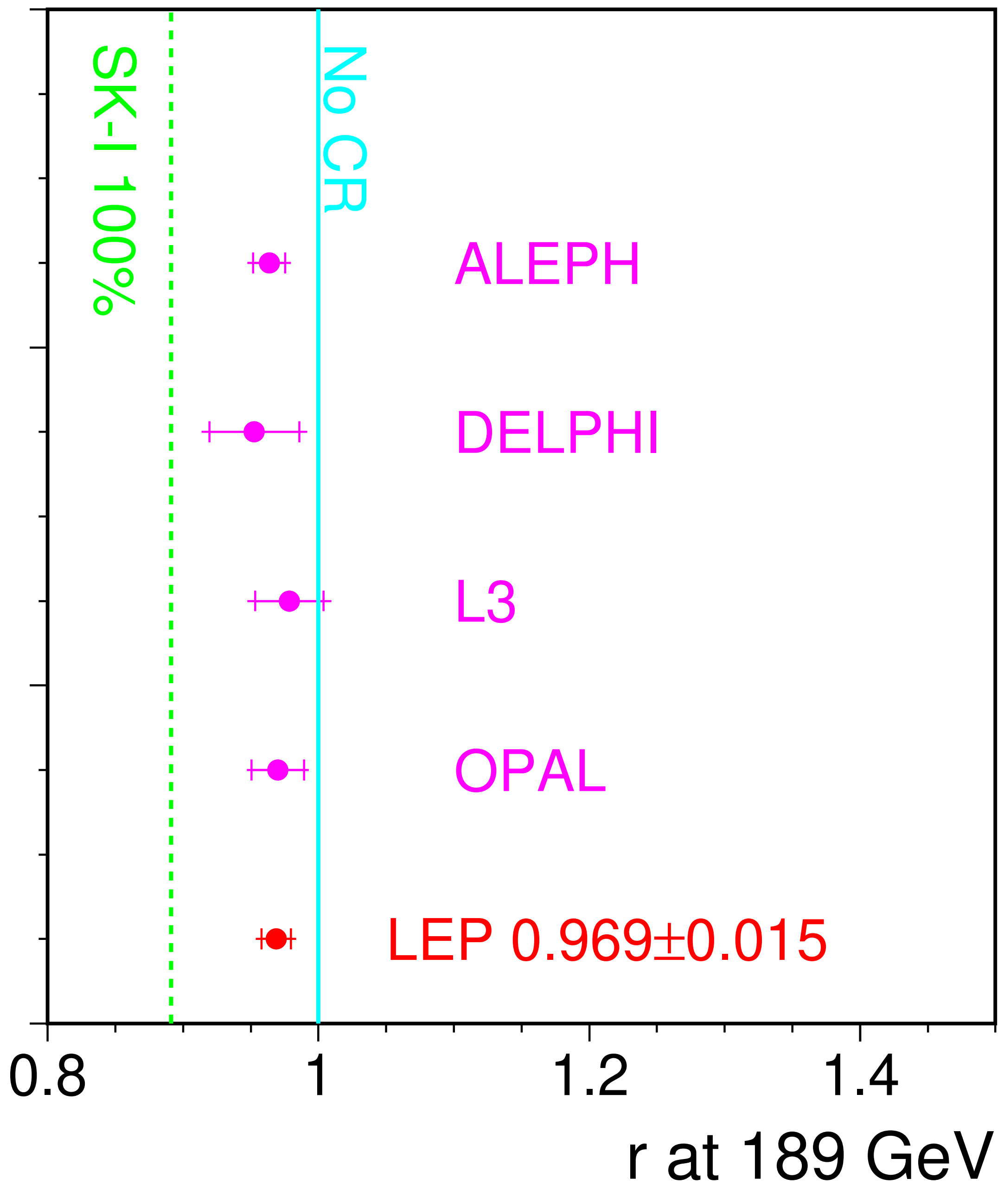

Figure 1: Preliminary particle flow results using all data, combined to test the limiting case of the SK-I model in which more than 99.9% of the events are colour reconnected. The error bar correspond to the total error with the inner part showing the statistical uncertainty.

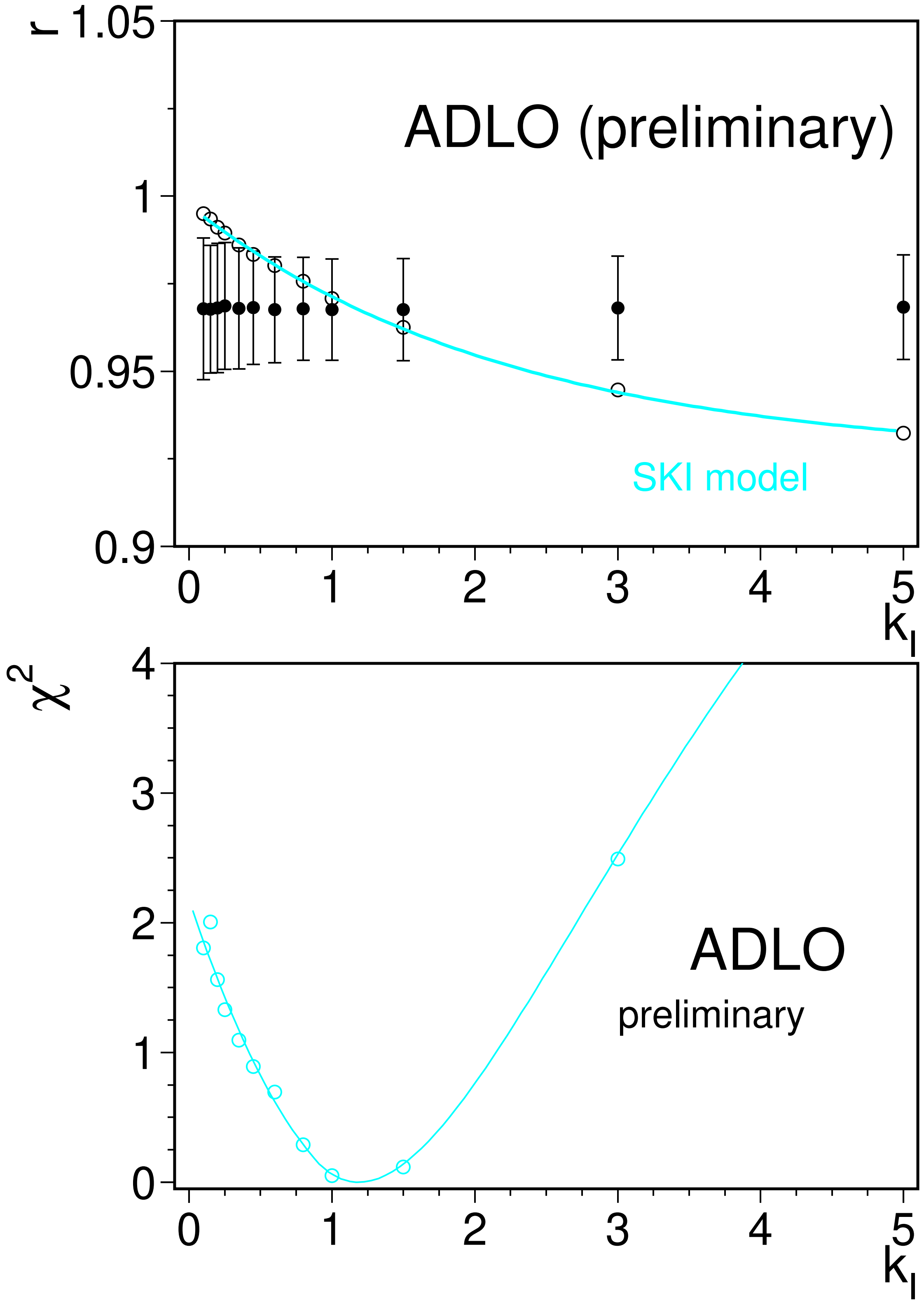

Figure 2: Comparison of the LEP average r values with the SKI model prediction obtained as a function of the k_I parameter. The MC line is a fit of a function of the form $r(k_I) = p_1(1 - exp(-p_2 k_I)) + p_3$. The bottom plot shows a χ^2 curve obtained from this comparison using all LEP data at the reference centre-of-mass energy of 189 GeV. The best agreement between the model and the data is obtained when $k_I = 1.18$.

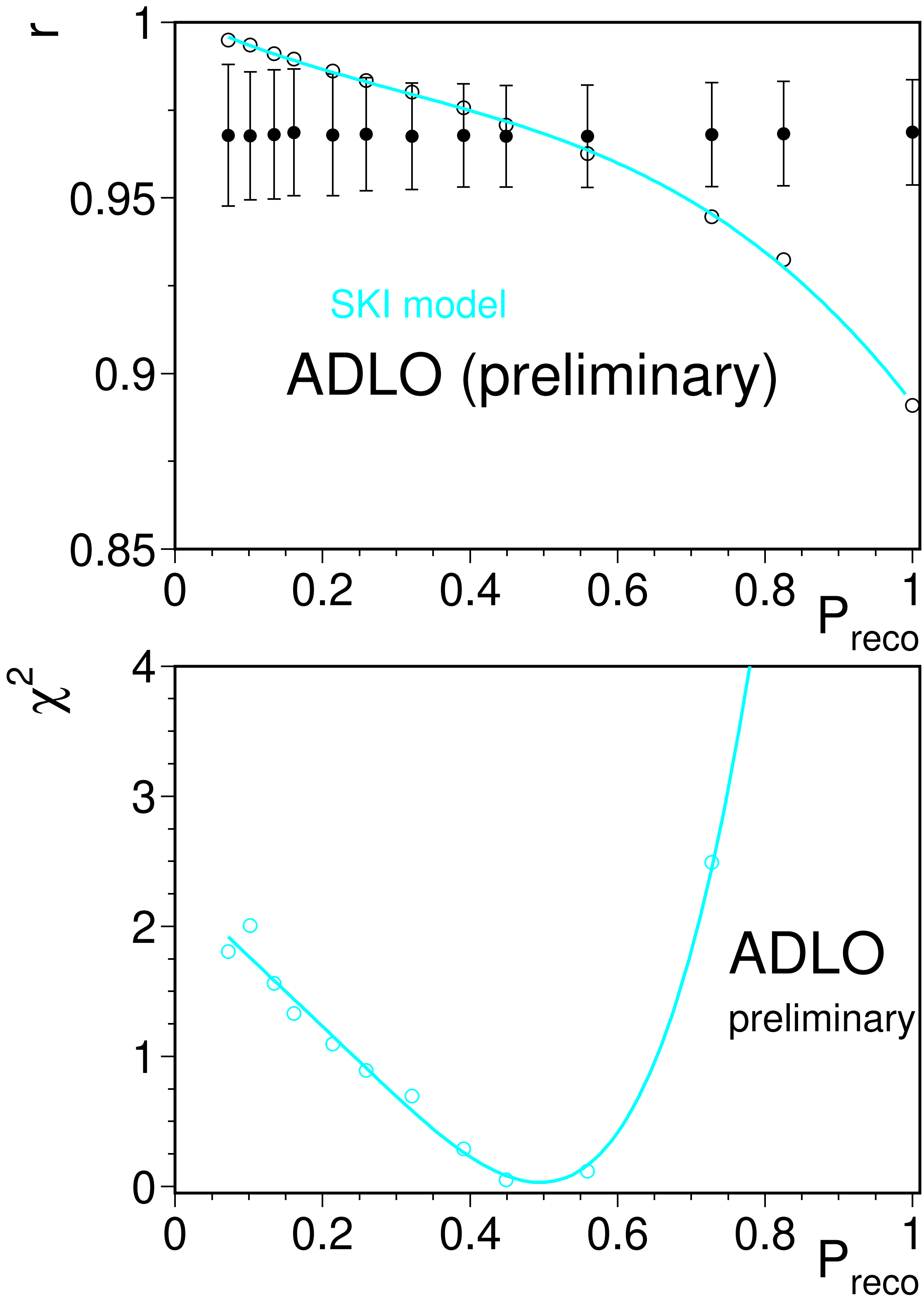

Figure 3: Comparison of the LEP average r values with the SKI model prediction obtained as a function of the reconnection probability. The MC line is obtained from a fit of a third order polynomial function. The bottom plot shows a χ^2 curve obtained from this comparison using all LEP data at the reference centre-of-mass energy of 189 GeV. The best agreement between the model and the data is obtained when 49% of events are reconnected in this model.

The observed variation of the LEP r average value and its corresponding error as a function of k_I (or P_{reco}) is essentially due to changes in the relative weighting of the experiments.

4.2 ARIADNE and HERWIG models

The combination procedure has been applied to common samples of ARIADNE and HERWIG Monte Carlo models. The R_N average values obtained with these models based on their respective predicted sensitivity are summarised in Table 5. The four experiments have observed a weak sensitivity to these colour reconnected samples with the particle flow analysis, as can be seen from Figure 4.

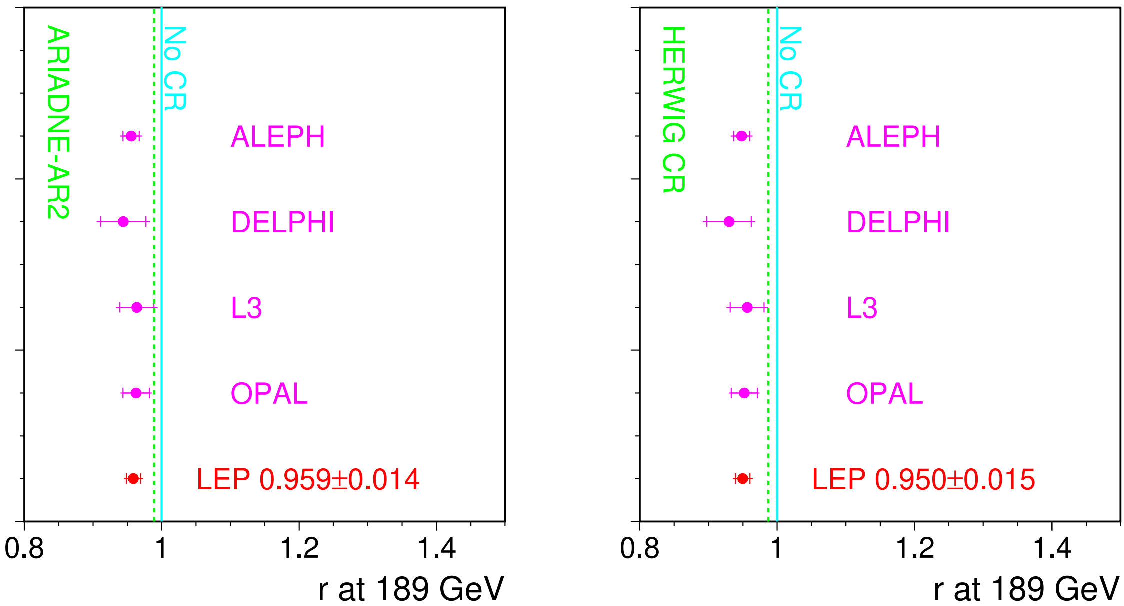

Figure 4: Preliminary particle flow results using all data, combined to test the ARIADNE and HERWIG colour reconnection models, based on the predicted sensitivity.

5 Summary

A first, preliminary combination of the LEP particle flow results is presented, using the total LEP2 data sample. The data disfavour by 5.2σ an extreme version of the SK-I model in which colour reconnection has been forced in basically all the events. The combination procedure has been generalised to the SK-I model as a function of its variable reconnection probability. The combined data favours the model where 49% of the events at 189 GeV are reconnected, corresponding to k_I =1.18. However the no colour reconnection is not ruled out. The LEP data deviates from this scheme by about 2σ. A 68% confidence level range has been determined for k_I and corresponds to [0.39,2.13].
The R_N values obtained with HERWIG and ARIADNE models, using the common Cetraro samples, differ from the measured data value by more than 2.6 and 2.1σ respectively. The differences between the results from the no CR and the colour reconnected scenario for these

two models are small and do not allow the particle flow analysis to discriminate between them. The observed deviations of the R_N values from all non-reconnected models may indicate a possible systematic effect in the description of particle flow for 4-jet events. Independent studies of particle flow in WW semileptonic events as well as other CR oriented analyses are required to investigate this.

References

[1] G. Gustafson, U. Pettersson, and P. M. Zerwas, Phys. Lett. **B209** (1988) 90.

[2] T. Sjostrand and V. A. Khoze, Z. Phys. **C62** (1994) 281–310.

[3] L. Lonnblad, Z. Phys. **C70** (1996) 107–114.

[4] G. Corcella *et al.*, JHEP **01** (2001) 010.

[5] G. Gustafson and J. Hakkinen, Z. Phys. **C64** (1994) 659–664.

[6] J. R. Ellis and K. Geiger, Phys. Rev. **D54** (1996) 1967–1990.

[7] J. Rathsman, Phys. Lett. **B452** (1999) 364–371.

[8] OPAL Collaboration, *Colour Reconnection Studies in* $\mathrm{e^+e^-} \rightarrow \mathrm{W^+W^-}$ *at* $\sqrt{s}$ *=189 GeV*, OPAL PN417.

[9] DELPHI Collaboration, P. Abreu *et al.*, Eur. Phys. J. **C18** (2000) 203–228.

[10] ALEPH Collaboration, *Preliminary Charged Particle Multiplicity in* $\mathrm{e^+e^-} \rightarrow$ *W-pairs*, ALEPH 2000-058 CONF 2000-038.

[11] L3 Collaboration, *Search for Colour Reconnection Effects in* $\mathrm{e^+e^-} \rightarrow \mathrm{W^+W^-} \rightarrow$ *hadrons*, L3 Note 2560.

[12] V. A. Khoze and T. Sjostrand, Eur. Phys. J. **C6** (1999) 271–284.

[13] OPAL Collaboration, *Investigation of Colour Reconnection via Heavy Particle Production in* $\mathrm{e^+e^-} \rightarrow \mathrm{W^+W^-}$, OPAL PN412.

[14] JADE Collaboration, W. Bartel *et al.*, Phys. Lett. **B101** (1981) 129;
JADE Collaboration, W. Bartel *et al.*, Z. Phys. **C21** (1983) 37;
JADE Collaboration, W. Bartel *et al.*, Phys. Lett. **B134** (1984) 275;
JADE Collaboration, W. Bartel *et al.*, Phys. Lett. **B157** (1985) 340;
TPC/Two Gamma Collaboration, H. Aihara *et al.*, Z. Phys. **C28** (1985) 31;
TPC/Two Gamma Collaboration, H. Aihara *et al.*, Phys. Rev. Lett. **57** (1986) 945;
TASSO Collaboration, M. Althoff *et al.*, Z. Phys. **C29** (1985) 29.

[15] L3 Collaboration, *Colour Reconnection Studies in* $\mathrm{e^+e^-} \rightarrow \mathrm{W^+W^-}$ *Events at* $\sqrt{s}$ = 189 *GeV*, L3 Note 2406.

[16] D. Duchesneau, *New Method Based on Energy and Particle Flow in* $\mathrm{e^+e^-} \rightarrow \mathrm{W^+W^-} \rightarrow$ *hadron Events for Colour Reconnection Studies*, LAPP-EXP-2000-02.

[17] A. Ballestrero *et al.*, J. Phys. **G24** (1998) 365–403.

[18] ALEPH Collaboration, *Colour Reconnection Studies Using Particle Flow Between W Bosons at* $\sqrt{s}$ *=189–208 GeV*, ALEPH 2002-020 CONF 2002-009.

[19] DELPHI Collaboration, *Update of the Investigation of Colour Reconnection in WW Pairs Using Particle Flow*, DELPHI 2002-047 CONF 581.

[20] L3 Collaboration, *Search for Colour Reconnection Effects in* $e^+e^- \to W^+W^- \to$ *hadrons Through Particle-Flow Studies at* $\sqrt{s}$ *=189–208 GeV*, L3 Note 2748.

[21] OPAL Collaboration, *Colour Reconnection Studies in* $e^+e^- \to W^+W^-$ *at* $\sqrt{s}$ *=189–208 GeV Using Particle Flow*, OPAL PN506.

[22] ALEPH Collaboration, R. Barate *et al.*, Eur. Phys. J. **C17** (2000) 241–261.

[23] OPAL Collaboration, G. Abbiendi *et al.*, Phys. Lett. **B507** (2001) 29–46.

[24] S. Jadach *et al.*, Comput. Phys. Commun. **140** (2001) 475–512.

[25] T. Sjostrand, Comput. Phys. Commun. **82** (1994) 74.

[26] L. Lonnblad, Comp. Phys. Comm. **71** (1992) 15.

[27] ALEPH Collaboration, *Further Studies on Bose-Einstein Correlations in W-pair Decays*, ALEPH 2001-064 CONF 2001-044.

[28] DELPHI Collaboration, *Particle Correlations in* $e^+e^- \to W^+W^-$ *Events*, DELPHI 2001-060 CONF 488.

[29] L3 Collaboration, *Measurements of Bose-Einstein Correlations in* $e^+e^- \to W^+W^-$ *Events at LEP*, L3 Note 2751.

[30] OPAL Collaboration, *Bose-Einstein Correlations in* $e^+e^- \to W^+W^-$ *Events at 172, 183 and 189 GeV*, OPAL PN393.

[31] A. Ballestrero *et al.*, *Report of the QCD working group*, Preprint hep-ph/0006259, CERN, 2000.

A Inputs

R_N	Experiment ALEPH	DELPHI	L3	OPAL
Data	1.0951 ± 0.0135	0.8996 ± 0.0314	0.8436 ± 0.0217	1.2570 ± 0.0251
SK-I (100%)	1.0548 ± 0.0012	0.8463 ± 0.0036	0.7482 ± 0.0033	1.1386 ± 0.0027
JETSET	1.1365 ± 0.0013	0.9444 ± 0.0039	0.8622 ± 0.0037	1.2958 ± 0.0028
AR-2	1.1341 ± 0.0013	0.9552 ± 0.0041	0.8696 ± 0.0037	1.2887 ± 0.0028
ARIADNE	1.1461 ± 0.0013	0.9530 ± 0.0039	0.8754 ± 0.0037	1.3057 ± 0.0028
HERWIG CR	1.1416 ± 0.0013	0.9649 ± 0.0039	0.8805 ± 0.0037	1.3016 ± 0.0029
HERWIG	1.1548 ± 0.0013	0.9675 ± 0.0040	0.8822 ± 0.0038	1.3204 ± 0.0029
Systematics				
Intra-W BEC	± 0.0020	± 0.0094	± 0.0017	± 0.0015
$e^+e^- \to q\bar{q}$ shape	± 0.0012	± 0.0013	± 0.0086	± 0.0035
$\pm 10\%$ $\sigma(e^+e^- \to q\bar{q})$	± 0.0036	± 0.0042	± 0.0071	± 0.0040
$\pm 15\%$ $\sigma(ZZ \to q\bar{q}q\bar{q})$	± 0.0004	± 0.0001	± 0.0020	± 0.0013
Detector effects	0.0040	–	± 0.0016	± 0.0072
E_{cm} dependence	± 0.0062	± 0.0012	± 0.0020	± 0.0030

Table 1: Inputs provided by the experiments for the combination.

B Example Average

k_i	P_{reco} (%)	ALEPH	DELPHI	L3	OPAL
0.10	7.2	1.1357 ± 0.0057	0.9410 ± 0.0034	0.8613 ± 0.0037	1.2887 ± 0.0028
0.15	10.2	1.1341 ± 0.0057	0.9393 ± 0.0032	0.8598 ± 0.0037	1.2859 ± 0.0028
0.20	13.4	1.1336 ± 0.0057	0.9378 ± 0.0031	0.8585 ± 0.0037	1.2823 ± 0.0028
0.25	16.1	1.1336 ± 0.0057	0.9363 ± 0.0030	0.8561 ± 0.0037	1.2800 ± 0.0028
0.35	21.4	1.1303 ± 0.0057	0.9334 ± 0.0028	0.8551 ± 0.0037	1.2741 ± 0.0028
0.45	25.9	1.1269 ± 0.0057	0.9307 ± 0.0027	0.8509 ± 0.0036	1.2693 ± 0.0028
0.60	32.1	1.1216 ± 0.0057	0.9271 ± 0.0025	0.8482 ± 0.0036	1.2639 ± 0.0028
0.80	39.1	1.1166 ± 0.0056	0.9227 ± 0.0024	0.8414 ± 0.0037	1.2576 ± 0.0028
1.00	44.9	1.1109 ± 0.0056	0.9189 ± 0.0024	0.8381 ± 0.0036	1.2499 ± 0.0028
1.50	55.9	1.1048 ± 0.0056	0.9110 ± 0.0025	0.8318 ± 0.0036	1.2368 ± 0.0028
3.00	72.8	1.0929 ± 0.0056	0.8959 ± 0.0028	0.8135 ± 0.0036	1.2093 ± 0.0027
5.00	82.5	1.0852 ± 0.0056	0.8846 ± 0.0030	0.7989 ± 0.0035	1.1920 ± 0.0022

Table 2: SKI Model predictions for R_N obtained with the common LEP samples at 189 GeV. The second column gives the fraction of reconnected events in the common samples obtained for the different choice of k_I values.

Model tested SK-I (100%)	Experiment ALEPH	DELPHI	L3	OPAL
R_N (no CR)	1.1365 ± 0.0013	0.9444 ± 0.0039	0.8622 ± 0.0037	1.2958 ± 0.0028
R_N (with CR)	1.0548 ± 0.0012	0.8463 ± 0.0036	0.7482 ± 0.0033	1.1386 ± 0.0027
weight	19.688	7.054	18.250	28.202
r ($\equiv R_N(\text{data})/R_N^{\text{no-CR}}$)				
Data	0.9636	0.9526	0.9784	0.9701
Stat. error	0.0119	0.0332	0.0252	0.0194
Syst. error	0.0110	0.0206	0.0180	0.0121
Uncorrel. syst.				
Background	0.0013	0.0035	0.0128	0.0029
Hadronisation	0.0000	0.0094	0.0086	0.0051
Intra-W BEC	0.0013	0.0099	0.0016	0.0000
Detector effects	0.0035	–	0.0019	0.0056
E_{cm} dependence	0.0055	0.0123	0.0023	0.0023
Total uncorr. error	0.0068	0.0187	0.0158	0.0084
Correl. syst.				
Background	0.0031	0.0031	0.0031	0.0031
Hadronisation	0.0081	0.0081	0.0081	0.0081
Intra-W BEC	0.0012	0.0012	0.0012	0.0012
Total correl. error	0.0087	0.0087	0.0087	0.0087

Table 3: Normalised results of particle flow analysis, based on the predicted SK-I 100% sensitivity.

k_i	P_{reco} (%)	$< R_N/R_N^{\text{no-CR}} >^{MC}$	$< R_N/R_N^{\text{no-CR}} >^{ADLO}$	data-MC (σ)
0.10	7.2	0.9950	$0.9679 \pm 0.0167 \pm 0.0087 \pm 0.0076$	-1.34
0.15	10.2	0.9935	$0.9677 \pm 0.0146 \pm 0.0087 \pm 0.0065$	-1.42
0.20	13.4	0.9911	$0.9681 \pm 0.0148 \pm 0.0087 \pm 0.0066$	-1.25
0.25	16.1	0.9895	$0.9687 \pm 0.0144 \pm 0.0087 \pm 0.0066$	-1.15
0.35	21.4	0.9861	$0.9680 \pm 0.0136 \pm 0.0087 \pm 0.0062$	-1.05
0.45	25.9	0.9834	$0.9681 \pm 0.0123 \pm 0.0087 \pm 0.0057$	-0.98
0.60	32.1	0.9802	$0.9676 \pm 0.0112 \pm 0.0087 \pm 0.0053$	-0.84
0.80	39.1	0.9757	$0.9678 \pm 0.0106 \pm 0.0087 \pm 0.0052$	-0.54
1.00	44.9	0.9708	$0.9676 \pm 0.0103 \pm 0.0087 \pm 0.0051$	-0.22
1.50	55.9	0.9626	$0.9676 \pm 0.0105 \pm 0.0087 \pm 0.0051$	+0.34
3.00	72.8	0.9447	$0.9680 \pm 0.0107 \pm 0.0087 \pm 0.0053$	+1.58
5.00	82.5	0.9324	$0.9683 \pm 0.0108 \pm 0.0087 \pm 0.0054$	+2.42
10000	100	0.8909	$0.9687 \pm 0.0108 \pm 0.0087 \pm 0.0057$	+5.20

Table 4: LEP Average for various k_I values in SKI model. The first uncertainty is statistical, the second corresponds to the correlated systematic error and the third corresponds to the uncorrelated systematic error.

Model	$< R_N/R_N^{\text{no-CR}} >^{MC}$	$< R_N/R_N^{\text{no-CR}} >^{ADLO}$	data-MC (σ)
AR2	0.9888	$0.9589 \pm 0.0101 \pm 0.0086 \pm 0.0050$	-2.10
HERWIG CR	0.9874	$0.9498 \pm 0.0105 \pm 0.0086 \pm 0.0052$	-2.59

Table 5: LEP Average for ARIADNE and HERWIG models with colour reconnection. The first uncertainty is statistical, the second corresponds to the correlated systematic error and the third corresponds to the uncorrelated systematic error.